Circ_0084927 promotes cervical carcinogenesis by sponging miR-1179 that suppresses CDK2, a cell cycle-related gene

Xinhua Qu
Yantai Affiliated Hospital, Binzhou Medical College
Liumei Zhu
Yantai Affiliated Hospital, Binzhou Medical College
Linlin Song
Yantai Affiliated Hospital, Binzhou Medical College
Shaohua Liu (591215843@qq.com)
Yantai Affiliated Hospital, Binzhou Medical College https://orcid.org/0000-0001-6672-2725

Primary research

Keywords: cervical cancer, circ_0084927, miR-1179, CDK2

Posted Date: April 29th, 2020

DOI: https://doi.org/10.21203/rs.3.rs-24972/v1

Version of Record: A version of this preprint was published on July 21st, 2020. See the published version at https://doi.org/10.1186/s12935-020-01417-2.

Abstract

Background: Cervical cancer (CC) is a highly malignant tumor. Evolving researches on CC have unveiled a concept that circRNA exerts important roles in CC progression. In this study, we mainly explored the role of a novel circRNA, circ_0084927, and its regulatory network in the development of CC.

Methods: qRT-PCR was applied to evaluate the expression of circ_0084927, miR-1179 and CDK2 mRNA in CC tissues and cells. Dual-luciferase reporting experiments and RNA immunoprecipitation (RIP) assay were conducted to validate the target relationship of miR-1179 with circ_0084927 and CDK2 mRNA. CCK-8 and BrdU assay was used to evaluate CC cell proliferation. The adhesion and apoptosis phenotypes of CC cells were measured by cell-matrix adhesion and caspase 3 activation assay. Flow cytometry was employed to detect CC cell cycle.

Results: Our results indicated that circ_0084927 was up-regulated in CC tissues and cells, and circ_0084927 silence inhibited CC cell proliferation and adhesion, while facilitating apoptosis as well as triggering cell cycle arrest. On the other hand, miR-1179 down-regulation appeared in CC tissues. Additionally, circ_0084927 abolished miR-1179's inhibitory effects on cell proliferation and adhesion. Our study showed that CDK2 was up-regulated in CC tissues and played a cancer-promoting role. Furthermore, miR-1179 directly targeted CDK2, thereby inhibiting CDK2's promotion on the malignant phenotypes of CC cells. circ_0084927 revoked the inhibitory effect of miR-1179 on CDK2 by sponging miR-1179.

Conclusion: Circ_0084927 promoted cervical carcinogenesis by sequestering miR-1179 that directly targeted CDK2. Our results shed light on the circ_0084927/miR-1179/CDK2 regulatory network that strengthened CC aggressiveness, providing novel candidate targets for CC treatment.

Background

CC is a highly malignant tumor that seriously threatens women's life. The estimated incidence rate of CC is 13.1 per 100,000 women, with Africa and China together accounting for a third of the global incidence [1]. Persistent human papillomavirus (HPV) infection has been considered to be the main cause of CC, so preventive vaccines have been developed to prevent HPV infection thus suppressing CC occurrence [1-3]. Although the HPV vaccine, screening and prevention reduce the incidence of CC, there is still a high incidence of CC [4, 5] [1, 2]. In addition, surgical treatment combined with chemotherapy or radiotherapy have improved the survival outcome of CC patients, but the treatment effect in high-risk patients has remained poor [6-8]. Immunotherapy researches have also provided a new potential treatment of CC [9]. However, because CC is prone to metastasis and recurrence, the mortality rate of patients with CC has been still high [10]. Hence, the exploration of new early treatment and diagnosis methods for CC is of extraordinary significance and vital importance to illuminate the underlying molecular mechanisms.

CircRNAs are a class of non-coding RNAs with covalently closed ring structures, which could avoid themselves being degraded by exonucleases [11]. circRNAs perform a variety of biological functions. In

recent years, increasing studies have showed that circRNAs are inextricably linked to the malignant process of many cancers [12-16]. Researches on CC have progressed in the past 5 years, and most of the circRNAs have been found to promote CC PMID: [17-19]. Emerging researches have suggested that multiple circRNAs are associated with the pathological process of CC [20-22]. Besides, it was shown that the up-regulation of certain circRNAs appeared in CC tissues [23]. Strikingly, reconstructive analysis of CC discovered a complicated circRNA-miRNA-mRNA regulatory network [24]. As mentioned above, research on the underlying molecular mechanisms of circRNAs in CC drew increasing attention. However, whether circ_0084927 plays a regulatory role in CC and how it works have not been investigated. Therefore, it is of a great value to investigate the role of circ_0084927 as well as its potential regulatory network in CC.

MiRNAs are a class of small endogenous non-coding RNAs that interact with the 3'UTR of a target gene through complementary base pairing. Recent studies have shown that miRNAs act as a tumor promoter or suppressor in the occurrence and development of CC PMID: [25-28]. MiR-1179's role in cancer biology has been preliminarily studied in recent years, and it was found to play an inhibitory role in several cancers including glioblastoma, gastric cancer as well as non-small-cell lung cancer [29-31]. Besides, studies on miR-1179 showed that the abnormal down-regulation of miR-1179 accelerated the malignant process of breast cancer and pancreatic cancer [32, 33]. However, it remains unclear whether miR-1179 exerts a role in the regulation of CC.

Cyclin dependent kinase 2 (CDK2) gene, locating on the 12q13.2 chromosome, consists of eight exons. As a member of the protein kinase family, CDK2 participates in the complicated regulation of eukaryotic cell division cycle [34]. A previous study uncovered that CDK2-related signaling pathways conferred complicated roles in several cancers PMID: [35]. A few studies have been conducted to study the tumor promoting role of CDK2 in CC PMID: [36-38]. Besides, a previous bioinformatics analysis authenticated that CDK2-related signaling pathways was involved in CC [39]. On the other hand, it was shown that CDK2 was a downstream target of some miRNAs in CC progression [40, 41]. However, whether CDK2 could be regulated by miR-1179 in CC has not been studied, and the interactome involving CDK2 and circRNA remains limitedly studied.

Based on the background introduction, our study mainly focused on exploring the role of circ_0084927 in the development of CC, as well as revealing the potential molecular mechanism and regulatory network of circ_0084927 in affecting CC. Our results showed that circ_0084927 promoted the occurrence of CC by sequestering the inhibitory effect of miR-1179 on CDK2.

Materials And Methods

Sample acquisition and Cell culture

CC tissue samples were collected from Yantai Affiliated Hospital of Binzhou Medical College, and the study protocols were approved by the Ethics Committee of Yantai Affiliated Hospital of Binzhou Medical College. CC cell lines (HeLa, CaSki, SW756 and C-33A) and normal cervical epithelial cell line (HcerEpic) were purchased from the BNBIO (Beijing, China). HeLa, C-33A, SW756 and CaSki cells were cultured under

5% CO_2 at 37 °C in RPMI-1640 medium (E600028; Sangon, Shanghai, China) with 10% fetal bovine serum (16140071; Gibco; Thermo Fisher Scientific, Inc., Waltham, MA, USA), 100 μg/ml streptomycin. HcerEpic cells were cultured under 5% CO_2 at 37 °C in MEM medium (E600024; Sangon, Shanghai, China) with 10% fetal bovine serum, 100 μg/ml streptomycin.

Cell transfection

The small interfering RNAs of circ_0084927 (si-circ_0084927) and CDK2 (si-CDK2), and a negative control siRNA (si-NC) were synthesized by GenePharma (Shanghai, China). miR-1179 control, miR-1179 negative control, miR-1179 mimic (for luciferase reporter gene assay) and miR-1179 inhibitor were purchased from RiboBio Co., Ltd. (Guangzhou, China). HeLa and C-33A cells were transfected with si-NC, miR-1179 inhibitor, si-circ_0084927, si-CDK2, miR-1179 inhibitor plus si-circ_0084927 or miR-1179 inhibitor plus si-CDK2 via Lipofectamine ™ 2000 (11668019; Thermo Fisher Scientific, Inc., Waltham, MA, USA) through lipofectin transfection method for 20 minutes. Cells were incubated for 2 days at 37 °C, then analyzed by qRT-PCR.

Subcellular location using a nuclei-cytoplasm fractionation method

The separation of nuclear and cytoplasmic fractions was conducted prior to nuclear and cytoplasmic RNA isolation using the PARIS kit (AM1921; Thermo Fisher Scientific, Waltham, Mass., USA). The isolated RNA products in nuclei and cytoplasm were analyzed by qRT-PCR. The expression of circ_0084927 and ESRP1 mRNA was detected in nuclei and cytoplasm. GAPDH was used as a reference control for cytoplasmic expression, and U2 was used as a reference control for nuclear expression.

qRT-PCR

We first used Trizol reagents (15596026; Thermo Fisher Scientific, Inc., Waltham, MA, USA) according to the instructions to isolate and detect total RNA from the tissue samples and cell lines. The obtained RNA was then reverse transcribed into cDNA. MiR-1179 was reverse transcribed following the protocol of mirVana™ qRT-PCR miRNA Detection Kit (AM1558; Invitrogen™; Thermo Fisher Scientific, Inc., Waltham, MA, USA). Reverse transcription CDK2 mRNA and circ_0084927 was conducted with SuperScript™ III First-Strand Synthesis SuperMix for qRT-PCR (; Thermo Fisher Scientific, Inc., Waltham, MA, USA). StepOnePlus™ Real-Time PCR System (4376600; Thermo Fisher Scientific, Inc., Waltham, MA, USA) was used to perform qRT-PCR. The qPCR products were validated using agarose gel electrophoresis method. The data were analyzed with $2^{-\Delta\Delta Ct}$ method. GAPDH was used as the internal control of circ_0084927 and CDK2 mRNA. U6 was used as the internal control of miR-1179

Luciferase reporter gene assay

Oligonucleotides comprising the circ_0084927 mutant (the sequence containing the miR-1179 binding site was mutated to GAUACGA) or the CDK2 mRNA 3'UTR mutant (the sequence containing the miR-1179 binding site was mutated to GAUACGA) were synthesized by GenePharma (Shanghai, China).

circ_0084927 wild type, circ_0084927 mutant, CDK2 3'UTR mutant and CDK2 wild-type were inserted into the Dual-Luciferase miRNA target expression vector (pGL4) to construct luciferase reporter plasmid. HeLa and C-33A cells were co-transfected with luciferase porter plasmid and miR-1179 mimic. After 48 hours of incubation, the culture medium was removed to collect the cells. The collected cells were lysed to collect cell lysates. The luciferase activity was measured by Pierce Renilla-Firefly Luciferase Dual Assay Kit (16185; Thermo Fisher Scientific, Inc., Waltham, MA, USA) according to the protocol.

RNA immunoprecipitation (RIP) assay

The Hela and C-33A cells transfected with miR-1179 mimic were cultured to an appropriate density. The cell culture was digested using trypsin and collected after trypsin treatment. The cells were lysed by RIP lysis buffer. Cell lysates were incubated with RIP buffer containing magnetic beads coupled with anti-Argonaute2 (MA5-23515; Thermo Fisher Scientific, Inc., Waltham, MA, USA) or IgG for 1 hour, with IgG as a negative control. The mixture was then incubated with Proteinase K. The immunoprecipitated RNA was isolated and analysed using qRT-PCR.

RNA pull-down assay

RNA pull-down assay was conducted to further validate the regulatory binding relationship between miR-1179 and CDK2 mRNA besides of the dual luciferase reporter gene assay. Firstly, Biotinylated double-stranded RNA of miR-1179 (Bio-miR-1179) and biotinylated negative control RNA (Bio-NC) were designed by GenePharma (Shanghai, China). The sense sequence of bio-miR-1179 was 5’-AAGCAUUCUUUCAUUGGUUGG-biotin-3’. The antisense sequence of bio-miR-1179 was 5’-CCAACCAAUGAAAGAAUGCUU-3’. 1×10^5 Hela and C-33A cells were cultured in 6-well plates for one day, resuspended in 1 mL lysis buffer, and incubated for 20 min on ice. The lysate was centrifuged at 12000×g for 15 min, and the supernatant was collected. The mixture of bio-miR-1179 or bio-NC and streptavidin-coated magnetic beads (Invitrogen, USA) was added to the supernatant for 2 hours incubation at 4°C. The pulled-down CDK2 mRNA in the bio-miR-1179 or bio-NC group was detected by RT-qPCR.

CCK-8 assay

After the transfected cells were trypsinized, 100 μl of the transfected cell suspension was seeded into a 96-well plate ($2x10^3$ cells/well). The plate after cell seeding is placed in a 37 °C incubator for the appropriate time (24 hours, 48 hours, and 72 hours). Then 10 μl of CCK-8 solution was added to each well according to the procedures in the manual of CCK-8. After the cells were incubated with CCK-8 for 2 hours, the absorbance was measured at 450 nm.

BrdU incorporation ELISA assay (A colorimetric BrdU assay)

BrdU cell proliferation detection kit was used to detect cell proliferation ability. Anti-BrdU antibodies were used to detect 5-bromo 2'-deoxyuridine (BrdU) incorporated into cell DNA during cell proliferation. Briefly,

trypsin-treated suspension containing 10^4 cells was added to each well of a 24-well plate. The culture medium was changed every 6 hours. After the cells were cultured for 24 hours, 10 μm BrdU (E607203; Sangon, Shanghai, China) was added, and the culturing was continued for 4 hours to allow the proliferating cells to incorporate BrdU into their DNA. The cultured cells were then fixed using the fixing solution, and permeabilized with 0.5% Triton (R) X-100 for 10 minutes. Mouse anti-IgG and anti-BrdU antibodies (diluted at 1:50) were incubated with the cells overnight at 4 °C. Subsequently, cells were washed with PBST and incubated with HRP-conjugated secondary antibodies (A24494; Thermo Fisher Scientific, Inc., Waltham, MA, USA) at 1:500 in PBS at room temperature in the dark. The absorbance at 450 nm was proportional to the amount of BrdU incorporated into the cell, which directly reflected cell proliferation.

Cell-matrix adhesion assay

Before the cell suspension (10,000 cells/well) was seeded in 96-well plates (4414133; Thermo Fisher Scientific, Inc., Waltham, MA, USA) previously coated with 10 μg/ml type I collagen (C7661, Sigma-Aldrich, USA), the cells were deprived from serum for at least 8 h. After 30 minutes to 1 hour adherence at 37˚C in a 5% CO_2 atmosphere, the wells were washed with PBS for at least three times to remove the non-adherent cells. The remaining cells were treated with MTT for an additional 2 h at 37 °C. Finally, the MTT-treated cells were treated with 100 μl DMSO. The absorbance at 570 nm was assessed at 570 nm using a microplate reader (Benchmark, Bio-Rad, U.S.A.).

Assays for caspase 3 activation

Caspase-3 is an active cell-apoptosis protease and an early indicator of the onset of apoptosis. Colorimetric detection at 405 nm of p-nitroaniline (pNA) after cleavage from the peptide substrate DEVD-pNA may reflect the cell apoptosis level. Briefly, the transfected Hela and C-33A cells ($1x10^5$) in different groups were harvested and lysed in 50 ml of ice-cold cell lysis buffer. Cell lysates were centrifuged at 10,000 g for 10 min to obtain the supernatant. Then 50 μl of 2x Reaction Buffer/DTT Mix and 5 μl of 1 mM DEVD-pNA (substrate for caspase-3) from caspase 3 colorimetric assay kit (630217, Takara Biomedical Technology (Beijing) Co., Ltd., China) were added to the cell lysates. determined by measuring OD405 of the released pNA using a microplate reader (Benchmark, Bio-Rad, U.S.A.).

Western blot analysis

Quantitative analysis was performed after total protein was extracted with RIPA lysis buffer (C500005, Sangon; Shanghai, China) from Hela and C-33A cells in different groups. An equal amount of protein was separated by 10% SDS-PAGE. The gel was immersed in a transfer buffer for equilibrium, and then transferred to a polyvinylidene fluoride membrane. Primary antibodies were diluted at a ratio of 1:1000. The membrane was incubated with diluted primary antibodies against CDK2 (D220395; Rabbit-Human; Sangon; Shanghai, China) and β-actin (SAB5500001; Rabbit-Human; Sigma-Aldrich, China) for 2 hours. The hybrid membrane was then blocked with 5% skimmed milk and incubated at 4 °C overnight. The membrane was subsequently incubated with diluted secondary antibodies (A32731; Goat-Rabbit; Thermo

Fisher Scientific, Inc., Waltham, MA, USA) for 2 hours. Finally, a hypersensitive ECL chemiluminescence kit (C510043; Sangon; Shanghai, China) was used to detect protein according to the reagent instructions. The intensity of the protein bands was read using ImageJ software.

Cell cycle by flow cytometry

The transfected HeLa and C-33A cells were resuspended once in pre-chilled 1xPBS, then were diluted to $1x10^5$ cells/ml in 1x Annexin binding buffer. 100 µl of cell suspension (10,000 cells) was used in every assay. Briefly, the transfected HeLa and C-33A cells were resuspended and treated with absolute ethanol for 30 minutes. Cells were then incubated with RNase for 30 minutes to remove RNA to eliminate the influence of the binding between PI and RNA. Cells were then stained with the red-fluorescent stain, PI (V13242; Thermo Fisher Scientific, Inc., Waltham, MA, USA), in a dark room at room temperature to allow PI to bind to DNA of cells. The stained cells were put into a flow cytometer, and the proportion of cells in each phase of the cell cycle was obtained from the linked BD FACSuite software.

Statistical analysis

All means and standard deviations were calculated based on three independent experiments using Microsoft Excel. GraphPad Prism 8.0 (GraphPad Prism, Inc., La Jolla, CA, USA) was used to produce the diagrams. One-factor analysis of variance (ANOVA) test was used for statistical analysis between multiple groups. Student's t test was used for statistical analysis of two groups. In terms of gene expression in tissue samples, we used Wilcoxon test for the CC tissue samples and matched adjacent healthy tissue samples comparision. $P< 0.05$ was considered to be statistically significant, and $P< 0.01$ was considered be extremely significant.

Results

Circ_0084927 was selected as the circRNA of interest in CC

By analysing the GSE102686 data series using GEO2R algorithm, we identified 21 differentially expressed genes (DEGs). Top 5 most significantly up-regulated circRNAs included circ_0084927, circ_0106385, circ_0099591, circ_0081723, and circ_0084912 (Figure 1A). Then we analyzed the expression of these five circRNAs in the obtained tissue samples. qRT-PCR results showed that except circ_0106385, circ_0084927, circ_0099591, circ_0081723, and circ_0084912 were significantly up-regulated in CC tissues than in paired healthy cervical tissues (Figure 2B-F). We selected circ_0084927, which had the second highest expression level, as the research object. Further analysis of circ_0084927 expression revealed that circ_0084927 was significantly up-regulated in CC cell lines including HeLa, CaSki, SW756 and C-33A compared to normal cervical epithelial cell line (HcerEpic). In particular, Hela and C-33A cell lines showed more than 2-fold circ_0084927 expression of HcerEpic cell line (Figure 2G), and were selected for follow-up studies. It was described that circ_0084927 was a closed circular RNA, generated from and contained exons 7, 8 and 9 of its host gene, ESRP1 (Figure 2H). To further characterize circ_0084927, we performed RNase R degradation experiments on HeLa and C-33A cells. The data

showed that RNase R greatly reduced linear_0084927 expression but had little effect on circ_0084927 expression in both cell lines (Figure 2I). In addition, subcellular fractionation location analysis of HeLa and C-33A cells suggested that circ_0084927 and linear_0084927 were mainly located in the cytoplasm (Figure 1J).

miR-1179 was identified as a bridge effector of circ_0084927 and CDK2 in CC

Metascape.org was firstly employed to analyse the enriched terms of 904 DEGs (selection criteria: adj. P<0.01 and log|FC|>=2) from of GSE63514 data series. As shown in a bar graph (Figure 2A), cell cycle was the most significantly enriched terms by Metascape.org algorithm. Particularly, critical genes that involved in cell cycle process in CC can be seen through an MCODE profile (Figure 2B). Then, we conducted a GSEA analysis of all genes in GSE63514 and found that cell cycle-related processes such as cell cycle, regulation of cell cycle phase transition, and cell cycle checkpoint process were all up-regulated in CC (Figure 2C). By intersecting the 904 DEGs of GSE63514 data series, genes that involved in the three cell cycle-related processes identified by GSEA analysis, 14 genes were identified (Figure 2D). The 14 genes then went through STRING v11 (https://string-db.org/) protein-protein interaction network analysis. As shown in the network, we noticed that CDK2 was significantly related with other proteins (Figure 2E). It was also known by us that CDK2 had been studied thoroughly in cervical cancer, however, its networking with circRNAs had been limitedly studied. Thus, CDK2 was chosen as our gene of interest in this study. By querying GEPIA expression data, we also found that CDK2 were significantly up-regulated in cervical squamous cancer (CESC) tissue samples (Figure 2F). We then intersected downstream miRNAs of circ_0084927 predicted by circular RNA interactome (https://circinteractome.nia.nih.gov/), and the upstream miRNAs of CDK2 mRNA predicted by TargetScan Human 7.2 (http://www.targetscan.org/vert_72/). Finally, miR-1179 was identified (Figure 1G). The relative expression of miR-1179 in our collected tissue samples was measured and it was found that miR-1179 was significantly downregulated in CC tissues rather than healthy control tissues (Figure 1H).

Circ_0084927 directly repressed miR-1179 by targeted inhibition

Circ_0084927 and miR-1179 were predicted to bind with each other via pairing in the GAAUGCU-CUUACGA manner (Figure 3A). To verify the interaction of circ_0084927 and miR-1179, we mutated the GAAUGCU sequence of circ_0084927 that bound to miR-1179 to GAUACGA. Luciferin-containing circ_0084927 mutant or circ_0084927 wild-type plasmids and miR-1179 mimic were co-transfected into HeLa and C-33A cells. It was showed that the introduction of miR-1179 mimic into the cells attenuated the luciferase expression of circ_0084927 wild-type plasmids, but had no effect on circ_0084927 mutant (Figure 3B). Besides, RIP results demonstrated that the addition of miR-1179 mimic precipitated circ_0084927 (Figure 3C). Moreover, miR-1179 expression displayed a negative correlation with circ_0084927 in CC tissues (Figure 3D). Lastly, miR-1179 was found to be significantly downregulated in CC cell lines. Hela and C-33A cell lines showed approximately ½ lower miR-1179 levels than HcerEpic cell line (Figure 3E).

Circ_0084927 promoted cervical carcinogenesis by inhibiting miR-1179

In order to investigate what role circ_0084927 plays through sponging miR-1179 in CC, we transfected circ_0084927 siRNA (si-circ_0084927), miR-1179 inhibitor or si-circ_0084927 plus miR-1179 inhibitor into HeLa and C-33A cells. si-circ_0084927 decreased circ_0084927 level while increased miR-1179 level. Meanwhile, miR-1179 inhibitor reduced miR-1179 but had no effect on circ_0084927 expression compared to the CON (control) group. In addition, si-circ_0084927 seemed to compromise the effects of miR-1179 inhibitor on miR-1197 expression, while miR-1179 inhibitor did not in turn affect the circ_0084927 expression (Figure 4A). The above results indicated that the HeLa and C-33A cells were successfully transfected. The results of subsequent CCK-8 and BrdU incorporation assays on the successfully transfected HeLa and C-33A cells displayed that the transfection of si-circ_0084927 declined cell proliferation, while the transfection of miR-1179 inhibitor stimulated it. Meanwhile, the proliferation of the HeLa and C-33A cells co-transfected with si-circ_0084927 and miR-1179 inhibitor had no significantly change compared with control, implying that their effects could be antagonized (Figure 4B-C). Furthermore, flow cytometry was employed to assess cell cycle progression. It was shown that si-circ_0084927 significantly increased the proportion of HeLa and C-33A cells in S phase (by approximately 25% in Hela cell line and 50% in C-33A cell line) but decreased the proportion in G2/M phase (by approximately 40% in Hela cell line and 40% in C-33A cell line). In contrast, miR-1179 inhibitor reduced the proportion of cells in S phase by approximately 30% in both cell lines, which was recovered by si-circ_0084927 (Figure 4D). Moreover, cell adhesion experiments showed that transfection with si-circ_0084927 reduced the cell's adhesion ability by a third compared to the control, while transfection with miR-1179 inhibitor increased the cell's adhesion ability by approximately 25% in both cell lines. At the same time, the decrease in cell adhesion ability caused by si-circ_0084927 could be restored by miR-1179 inhibitor transfection (Figure 4E). Caspase 3 is usually activated during apoptosis, irrespective of the specific death-initiating stimulus [42, 43], thus could reflect the cell apoptosis level. According to caspase 3 activation assay, it was shown that the apoptosis of HeLa and C-33A cells was significantly facilitated by circ_0084927 silence, increased by over 5-fold, but repressed by miR-1179 inhibition, decreased by around a half. In the meantime, increased apoptosis caused by si-circ_0084927 was compromised by miR-1179 inhibition (Figure 4F).

MiR-1179 directly targeted CDK2 mRNA by binding to its 3'UTR

It's predicted that miR-1179 paired with the 205-211 position of the 3'UTR of the CDK2 mRNA (Figure 5A). Detection of the luciferase intensities demonstrated that the introduction of miR-1179 mimic decreased the fluorescence intensity of cells transfected with CDK2 wild-type plasmids but not the cells transfected with CDK2 mutant (Figure 5B). On the other hand, RNA pull-down experiment results also showed that miR-1179 interacted with CDK2 mRNA (Figure 5C). We subsequently analyzed CDK2 mRNA level in the obtained tissue samples, indicating that CDK2 was up-regulated in CC tissues (Figure 5D). Besides, it was shown that miR-1179 was negatively correlated with CDK2 expression (Figure 5E).

Circ_0084927 promoted cervical carcinogenesis by sponging miR-1179 that suppressed CDK2

To identify the effect of CDK2 expression in CC, we transfected CDK2 siRNA (si-CDK2) or miR-1179 inhibitor into HeLa and C-33A cells. At the same time, miR-1179 inhibitor and si-CDK2 were co-transfected into HeLa and C-33A cells to neutralize each other's effects on CDK2 expression. qRT-PCR analysis (results in Figure 6A) of transfected cells exhibited that compared with the control group, transfection of si-CDK2 reduced CDK2 mRNA, while transfection of miR-1179 inhibitor increased it. Besides, the reduction of CDK2 mRNA caused by si-CDK2 was restored by miR-1179 inhibitor, indicating that the cells were successfully transfected. The efficiency of si-CDK2 reached approximately 70%. Western blotting analysis of CDK2 also demonstrated successful transfection at protein level (Figure 6B). The next step of our research was to explore the cellular phenotypes of successfully transfected HeLa and C-33A cells. According to the results of CCK-8 assay, it could be seen that silencing CDK2 attenuated HeLa and C-33A cell proliferation, while miR-1179 down-regulation offset the inhibitory effect caused by CDK2 silence at 48 h and 72 h (Figure 6C). Equally, BrdU experiment showed the same cell proliferation results that CDK2 silencing inhibited cell proliferation (Figure 6D). In addition, silencing CDK2 significantly increased the proportion of S-phase cells compared to the control but decreased the proportion at G1 phase. Besides, the increase in the proportion of S-phase cells caused by CDK2 silencing was attenuated by the down-regulation of miR-1179 (Figure 6E). CDK2 silencing significantly reduced HeLa and C-33A cell adhesion, and this reduction was restored by simultaneous down-regulation of miR-1179 (Figure 6F). Finally, in caspase 3 activation experiments, CDK2 silencing increased HeLa and C-33A cell apoptosis, which was compromised by miR-1179 down-regulation (Figure 6G).

Discussion

In our research, it was proved that circ_0084927 silencing inhibited carcinogenesis by repressing the proliferation and adhesion of CC cells, fortifying apoptosis as well as leading to cell cycle arrest. Collectively, circ_0084927 promoted the occurrence of CC through the regulatory network of circ_0084927/miR-1179/CDK2.

There have been accumulating studies reporting the up-regulation and miRNA-sponging roles of circRNAs in CC, a family of circular non-coding RNAs. For instance, circ_101996 was over-expressed in cervical cancerous tissues [44]. A previous study showed that circ_0084927 was significantly up-regulated in malignant pleural effusion (MPE) of lung cancer [45]. Herein we reported the significant up-regulation of circ_0084927 in CC tissues and cell lines. It was hypothesized that the upregulated circ_0084927 might facilitate CC progression.

Many up-regulated circRNAs were reported to exert critical tumor promoting functions by sponging its downstream miRNAs. For instance, circ_0023404 and hsa_circ_CLK3 stimulated the aggressiveness of CC cells through acting as sponge of miRNAs, thereby facilitating cancer occurrence and metastasis [46, 47]. What’s more, circ_0000515 served as a miR-326 sponge to promote the progression of CC PMID: [18, 48]. According to a recent study, up-regulated circ_0000388 dramatically stimulated CC aggression through sponging miR-337-3p [49]. circ_0075341 was identified as a sponge of miR-149-5p to promote the malignant phenotypes of CC cells [19]. In another study, circ_0060467 stimulated aggressiveness of

CC by sponging miR-361-3p [50]. We herein identified a potential downstream miRNA of circ_0084927, miR-1179, which has been limitedly studied in several cancers except CC. We found that circ_0084927 promoted CC malignant phenotypes by sponging miR-1197, suggesting that circ_0084927 also exerted its tumor-promoting functions by suppressing miR-1197. In terms of miR-1197, it was once described as a tumor suppressor that impaired the malignant progression of gastric cancer by inhibiting proliferation and invasion [30]. Another study showed that increased miR-1179 significantly inhibited the aggressiveness of breast cancer cells while at the same time weakening the cancer metastasis [33]. Moreover, miR-1179 behaved as a tumor suppressor to inhibit the malignant proliferation and cell cycle progression of glioblastoma multiforme cells [29]. Above all, it has been suggested that miR-1179 could be a potential tumor suppressor in diverse cancers. However, no previous studies showing that miR-1179 also played a tumor suppressor role have been reported in CC. We here supplemented the results in CC and proposed that miR-1179 played an anti-oncogenic role in CC. It's worth noticing that miR-1179 has been reported to interact with other circRNAs thus affecting human cancer cell phenotypes. For instance, it was described in a previous study that the tumor suppressor function of miR-1179 was confiscated by circ_0000735 during the development of non-small cell lung cancer [51]. A similar exploration testified that the inhibitory effect of miR-1179 on thyroid cancer was sponged by circ_0039411 during the pathological process [52]. Another study pointed out that circ_0003645 improved cell aggressiveness through sponge of miR-1179 [53]. In addition, circ_0025033 as a cancer-promoting factor promoted the progression and tumor growth of papillary thyroid carcinoma by sponging miR-1179 [54]. These studies supported the opinion that miR-1179 could exert tumor suppressor functions by sponging with circRNAs. Our study validated the regulatory relationship between circ_0084927 and miR-1179. Our findings not only unraveled the tumor promoting effect of circ_0084927, but also expanded the regulatory networking involving miR-1179 in CC. We identified a novel regulatory interactome that might contribute to the comprehension of CC pathogenesis.

Regarding the downstream effector of miR-1179, CDK2, several studies have reported that CDK2 is the downstream effector of miRNAs in a variety of cancers thereby affecting cancer cell malignancy especially cell cycle progression. For instance, silencing CDK2 attenuated aerobic glycolytic cell metabolism in cells, thereby inhibiting the malignant characterization of gastric cancer cells [55]. What's more, CDK2 was up-regulated in many cancers as a cell cycle-dependent kinase that normally contributed to cell cycle progression and DNA damage responses [56]. This up-regulation of CDK2 provided new immune targets for therapy on multiple cancers, and the study of CDK2 inhibitors also provided new prospects for cancer treatment [57, 58]. Our results showed that the inhibition of CDK2 significantly suppressed CC cell growth and cell cycle progression as well as call-matrix adhesion. Consistent with previous studies, our study also indicated that CDK2 could be a valuable therapy target for CC treatment. In terms of the interaction miRNAs and circRNAs that are upstream of CDK2, it was reported that, by downregulating by miR-3619-5p, CDK2 exerted a crucial role in promoting the proliferation, migration and invasion of bladder carcinoma cells [59]. By regulating by its upstream circ_0078710/miR-31, CDK2 stimulated the malignant phenotypes of hepatocellular carcinoma cells [60]. Interestingly, CDK2 was pointed out to form a complex with circ-Foxo3 that was abnormally expressed in cancer tissues to

participate in cell cycle regulation [61]. The above evidences indicated that CDK2 could be downstream effectors of circNRAs and miRNAs. In our study, we reported a novel upstream regulator of CDK2, circ_0084927/miR-1179 in CC. miR-1179 inhibited the malignant phenotypes including cell cycle progression of CC cells by directly targeting CDK2, and this regulation could be reversed by circ_0084927 because it could sponge miR-1179 to release CDK2.

In order to better clarify the pathogenesis of CC, the results of the in vitro experiments in this study require the validation in animal models. Clinical samples need to be further accumulated to expand the sample size and make the results more convincing. Our study did not further investigate the molecular receptors downstream of the CDK2 in CC.

Conclusion

In summary, this study indicated that circ_0084927 stimulated CC by sponging miR-1179, which negatively targeted CDK2. Our results revealed the existence of a complex circ_0084927/miR-1179/CDK2 axis in cervical carcinogenesis. In terms of the search for CC therapy, our study highlighted the possibility of circ_0084927 as a candidate target.

Abbreviations

miRNAs: microRNAs; PBS: phosphate bufered solution; EdU: 5-ethynyl-2'-deoxyuridine; CC: cervical cancer; qPCR: quantitative real-time PCR.

Declarations

Ethics approval and consent to participate

Ethic Committee of The Yantai Affiliated Hospital of Binzhou Medical College (Shandong, China) approved the study.

Consent for publication

Informed consent was obtained from all patients.

Availability of Data and Materials

The datasets used during the current study are available from the corresponding author on reasonable request.

Funding

This research has received no funds.

Competing interests

There is no conflict of interest existed among the authors.

Authors' contributions

SHL designed the experiments. XHQ and LMZ conducted the experiments. LLS wrote the manuscript.

Acknowledgements

Not applicable.

References

1. Arbyn M, Weiderpass E, Bruni L, de Sanjose S, Saraiya M, Ferlay J, Bray F: **Estimates of incidence and mortality of cervical cancer in 2018: a worldwide analysis**. *Lancet Glob Health* 2020, **8**(2):e191-e203.
2. Brisson M, Kim JJ, Canfell K, Drolet M, Gingras G, Burger EA, Martin D, Simms KT, Benard E, Boily MC *et al*: **Impact of HPV vaccination and cervical screening on cervical cancer elimination: a comparative modelling analysis in 78 low-income and lower-middle-income countries**. *Lancet* 2020, **395**(10224):575-590.
3. Zapatka M, Borozan I, Brewer DS, Iskar M, Grundhoff A, Alawi M, Desai N, Sultmann H, Moch H, Pathogens P *et al*: **The landscape of viral associations in human cancers**. *Nat Genet* 2020, **52**(3):320-330.
4. Wang R, Pan W, Jin L, Huang W, Li Y, Wu D, Gao C, Ma D, Liao S: **Human papillomavirus vaccine against cervical cancer: Opportunity and challenge**. *Cancer Lett* 2020, **471**:88-102.
5. Chinn J, Tewari KS: **Multimodality screening and prevention of cervical cancer in sub-Saharan Africa: a collaborative model**. *Curr Opin Obstet Gynecol* 2020, **32**(1):28-35.
6. Hill EK: **Updates in Cervical Cancer Treatment**. *Clin Obstet Gynecol* 2020, **63**(1):3-11.
7. Lapresa M, Parma G, Portuesi R, Colombo N: **Neoadjuvant chemotherapy in cervical cancer: an update**. *Expert Rev Anticancer Ther* 2015, **15**(10):1171-1181.
8. Vordermark D: **Radiotherapy of Cervical Cancer**. *Oncol Res Treat* 2016, **39**(9):516-520.
9. Ventriglia J, Paciolla I, Pisano C, Cecere SC, Di Napoli M, Tambaro R, Califano D, Losito S, Scognamiglio G, Setola SV *et al*: **Immunotherapy in ovarian, endometrial and cervical cancer: State of the art and future perspectives**. *Cancer Treat Rev* 2017, **59**:109-116.
10. Li H, Wu X, Cheng X: **Advances in diagnosis and treatment of metastatic cervical cancer**. *J Gynecol Oncol* 2016, **27**(4):e43.
11. Kapranov P, Cawley SE, Drenkow J, Bekiranov S, Strausberg RL, Fodor SP, Gingeras TR: **Large-scale transcriptional activity in chromosomes 21 and 22**. *Science* 2002, **296**(5569):916-919.
12. Hsiao KY, Lin YC, Gupta SK, Chang N, Yen L, Sun HS, Tsai SJ: **Noncoding Effects of Circular RNA CCDC66 Promote Colon Cancer Growth and Metastasis**. *Cancer Res* 2017, **77**(9):2339-2350.

13. Hu ZQ, Zhou SL, Li J, Zhou ZJ, Wang PC, Xin HY, Mao L, Luo CB, Yu SY, Huang XW *et al*: **Circular RNA Sequencing Identifies CircASAP1 as a Key Regulator in Hepatocellular Carcinoma Metastasis**. *Hepatology* 2019.
14. Zhang PF, Pei X, Li KS, Jin LN, Wang F, Wu J, Zhang XM: **Circular RNA circFGFR1 promotes progression and anti-PD-1 resistance by sponging miR-381-3p in non-small cell lung cancer cells**. *Mol Cancer* 2019, **18**(1):179.
15. Xue D, Wang H, Chen Y, Shen D, Lu J, Wang M, Zebibula A, Xu L, Wu H, Li G *et al*: **Circ-AKT3 inhibits clear cell renal cell carcinoma metastasis via altering miR-296-3p/E-cadherin signals**. *Mol Cancer* 2019, **18**(1):151.
16. Huang X, He M, Huang S, Lin R, Zhan M, Yang D, Shen H, Xu S, Cheng W, Yu J *et al*: **Circular RNA circERBB2 promotes gallbladder cancer progression by regulating PA2G4-dependent rDNA transcription**. *Mol Cancer* 2019, **18**(1):166.
17. Cai H, Zhang P, Xu M, Yan L, Liu N, Wu X: **Circular RNA hsa_circ_0000263 participates in cervical cancer development by regulating target gene of miR-150-5p**. *J Cell Physiol* 2019, **234**(7):11391-11400.
18. Tang Q, Chen Z, Zhao L, Xu H: **Circular RNA hsa_circ_0000515 acts as a miR-326 sponge to promote cervical cancer progression through up-regulation of ELK1**. *Aging (Albany NY)* 2019, **11**(22):9982-9999.
19. Shao S, Wang C, Wang S, Zhang H, Zhang Y: **Hsa_circ_0075341 is up-regulated and exerts oncogenic properties by sponging miR-149-5p in cervical cancer**. *Biomed Pharmacother* 2020, **121**:109582.
20. Wang H, Zhao Y, Chen M, Cui J: **Identification of Novel Long Non-coding and Circular RNAs in Human Papillomavirus-Mediated Cervical Cancer**. *Front Microbiol* 2017, **8**:1720.
21. Ma HB, Yao YN, Yu JJ, Chen XX, Li HF: **Extensive profiling of circular RNAs and the potential regulatory role of circRNA-000284 in cell proliferation and invasion of cervical cancer via sponging miR-506**. *Am J Transl Res* 2018, **10**(2):592-604.
22. Hu C, Wang Y, Li A, Zhang J, Xue F, Zhu L: **Overexpressed circ_0067934 acts as an oncogene to facilitate cervical cancer progression via the miR-545/EIF3C axis**. *J Cell Physiol* 2019, **234**(6):9225-9232.
23. Li S, Teng S, Xu J, Su G, Zhang Y, Zhao J, Zhang S, Wang H, Qin W, Lu ZJ *et al*: **Microarray is an efficient tool for circRNA profiling**. *Brief Bioinform* 2019, **20**(4):1420-1433.
24. Yi Y, Liu Y, Wu W, Wu K, Zhang W: **Reconstruction and analysis of circRNAmiRNAmRNA network in the pathology of cervical cancer**. *Oncol Rep* 2019, **41**(4):2209-2225.
25. Wei WF, Zhou CF, Wu XG, He LN, Wu LF, Chen XJ, Yan RM, Zhong M, Yu YH, Liang L *et al*: **MicroRNA-221-3p, a TWIST2 target, promotes cervical cancer metastasis by directly targeting THBS2**. *Cell Death Dis* 2017, **8**(12):3220.
26. Hou T, Ou J, Zhao X, Huang X, Huang Y, Zhang Y: **MicroRNA-196a promotes cervical cancer proliferation through the regulation of FOXO1 and p27Kip1**. *Br J Cancer* 2014, **110**(5):1260-1268.

27. Chandrasekaran KS, Sathyanarayanan A, Karunagaran D: **MicroRNA-214 suppresses growth, migration and invasion through a novel target, high mobility group AT-hook 1, in human cervical and colorectal cancer cells**. *Br J Cancer* 2016, **115**(6):741-751.

28. Zhang P, Kong F, Deng X, Yu Y, Hou C, Liang T, Zhu L: **MicroRNA-326 suppresses the proliferation, migration and invasion of cervical cancer cells by targeting ELK1**. *Oncol Lett* 2017, **13**(5):2949-2956.

29. Xu X, Cai N, Zhi T, Bao Z, Wang D, Liu Y, Jiang K, Fan L, Ji J, Liu N: **MicroRNA-1179 inhibits glioblastoma cell proliferation and cell cycle progression via directly targeting E2F transcription factor 5**. *Am J Cancer Res* 2017, **7**(8):1680-1692.

30. Li Y, Qin C: **MiR-1179 inhibits the proliferation of gastric cancer cells by targeting HMGB1**. *Hum Cell* 2019, **32**(3):352-359.

31. Heller G, Altenberger C, Steiner I, Topakian T, Ziegler B, Tomasich E, Lang G, End-Pfutzenreuter A, Zehetmayer S, Dome B *et al*: **DNA methylation of microRNA-coding genes in non-small-cell lung cancer patients**. *J Pathol* 2018, **245**(4):387-398.

32. Lin C, Hu Z, Yuan G, Su H, Zeng Y, Guo Z, Zhong F, Jiang K, He S: **MicroRNA-1179 inhibits the proliferation, migration and invasion of human pancreatic cancer cells by targeting E2F5**. *Chem Biol Interact* 2018, **291**:65-71.

33. Li WJ, Xie XX, Bai J, Wang C, Zhao L, Jiang DQ: **Increased expression of miR-1179 inhibits breast cancer cell metastasis by modulating Notch signaling pathway and correlates with favorable prognosis**. *Eur Rev Med Pharmacol Sci* 2018, **22**(23):8374-8382.

34. Saurus P, Kuusela S, Dumont V, Lehtonen E, Fogarty CL, Lassenius MI, Forsblom C, Lehto M, Saleem MA, Groop PH *et al*: **Cyclin-dependent kinase 2 protects podocytes from apoptosis**. *Sci Rep* 2016, **6**:21664.

35. Bonin S, Pracella D, Barbazza R, Dotti I, Boffo S, Stanta G: **PI3K/AKT Signaling in Breast Cancer Molecular Subtyping and Lymph Node Involvement**. *Dis Markers* 2019, **2019**:7832376.

36. Abd El-Karim SS, Syam YM, El Kerdawy AM, Abdelghany TM: **New thiazol-hydrazono-coumarin hybrids targeting human cervical cancer cells: Synthesis, CDK2 inhibition, QSAR and molecular docking studies**. *Bioorg Chem* 2019, **86**:80-96.

37. Guo JM, Xiao BX, Liu Q, Zhang S, Liu DH, Gong ZH: **Anticancer effect of aloe-emodin on cervical cancer cells involves G2/M arrest and induction of differentiation**. *Acta Pharmacol Sin* 2007, **28**(12):1991-1995.

38. Choi JS, Shin S, Jin YH, Yim H, Koo KT, Chun KH, Oh YT, Lee WH, Lee SK: **Cyclin-dependent protein kinase 2 activity is required for mitochondrial translocation of Bax and disruption of mitochondrial transmembrane potential during etoposide-induced apoptosis**. *Apoptosis* 2007, **12**(7):1229-1241.

39. Wu K, Yi Y, Liu F, Wu W, Chen Y, Zhang W: **Identification of key pathways and genes in the progression of cervical cancer using bioinformatics analysis**. *Oncol Lett* 2018, **16**(1):1003-1009.

40. Tian RQ, Wang XH, Hou LJ, Jia WH, Yang Q, Li YX, Liu M, Li X, Tang H: **MicroRNA-372 is down-regulated and targets cyclin-dependent kinase 2 (CDK2) and cyclin A1 in human cervical cancer, which may contribute to tumorigenesis**. *J Biol Chem* 2011, **286**(29):25556-25563.

41. Duan S, Wu A, Chen Z, Yang Y, Liu L, Shu Q: **miR-204 Regulates Cell Proliferation and Invasion by Targeting EphB2 in Human Cervical Cancer**. *Oncol Res* 2018, **26**(5):713-723.
42. Luthi AU, Martin SJ: **The CASBAH: a searchable database of caspase substrates**. *Cell Death Differ* 2007, **14**(4):641-650.
43. Timmer JC, Salvesen GS: **Caspase substrates**. *Cell Death Differ* 2007, **14**(1):66-72.
44. Song T, Xu A, Zhang Z, Gao F, Zhao L, Chen X, Gao J, Kong X: **CircRNA hsa_circRNA_101996 increases cervical cancer proliferation and invasion through activating TPX2 expression by restraining miR-8075**. *J Cell Physiol* 2019, **234**(8):14296-14305.
45. Wen Y, Wang Y, Xing Z, Liu Z, Hou Z: **Microarray expression profile and analysis of circular RNA regulatory network in malignant pleural effusion**. *Cell Cycle* 2018, **17**(24):2819-2832.
46. Zhang J, Zhao X, Zhang J, Zheng X, Li F: **Circular RNA hsa_circ_0023404 exerts an oncogenic role in cervical cancer through regulating miR-136/TFCP2/YAP pathway**. *Biochem Biophys Res Commun* 2018, **501**(2):428-433.
47. Hong H, Zhu H, Zhao S, Wang K, Zhang N, Tian Y, Li Y, Wang Y, Lv X, Wei T *et al*: **The novel circCLK3/miR-320a/FoxM1 axis promotes cervical cancer progression**. *Cell Death Dis* 2019, **10**(12):950.
48. Tang Q, Chen Z, Zhao L: **Correction for: Circular RNA hsa_circ_0000515 acts as a miR-326 sponge to promote cervical cancer progression through up-regulation of ELK1**. *Aging (Albany NY)* 2020, **12**(4):4040.
49. Meng QH, Li Y, Kong C, Gao XM, Jiang XJ: **Circ_0000388 Exerts Oncogenic Function in Cervical Cancer Cells by Regulating miR-337-3p/TCF12 Axis**. *Cancer Biother Radiopharm* 2020.
50. Wang J, Li H, Liang Z: **circ-MYBL2 Serves As A Sponge For miR-361-3p Promoting Cervical Cancer Cells Proliferation And Invasion**. *Onco Targets Ther* 2019, **12**:9957-9964.
51. Li W, Jiang W, Liu T, Lv J, Guan J: **Enhanced expression of circ_0000735 forecasts clinical severity in NSCLC and promotes cell progression via sponging miR-1179 and miR-1182**. *Biochem Biophys Res Commun* 2019, **510**(3):467-471.
52. Yang Y, Ding L, Li Y, Xuan C: **Hsa_circ_0039411 promotes tumorigenesis and progression of papillary thyroid cancer by miR-1179/ABCA9 and miR-1205/MTA1 signaling pathways**. *J Cell Physiol* 2020, **235**(2):1321-1329.
53. An J, Shi H, Zhang N, Song S: **Elevation of circular RNA circ_0003645 forecasts unfavorable prognosis and facilitates cell progression via miR-1179/TMEM14A pathway in non-small cell lung cancer**. *Biochem Biophys Res Commun* 2019, **511**(4):921-925.
54. Ye M, Hou H, Shen M, Dong S, Zhang T: **Circular RNA circFOXM1 Plays a Role in Papillary Thyroid Carcinoma by Sponging miR-1179 and Regulating HMGB1 Expression**. *Mol Ther Nucleic Acids* 2020, **19**:741-750.
55. Tang Z, Li L, Tang Y, Xie D, Wu K, Wei W, Xiao Q: **CDK2 positively regulates aerobic glycolysis by suppressing SIRT5 in gastric cancer**. *Cancer Sci* 2018, **109**(8):2590-2598.

56. Chen Y, Du J, Wang Y, Shi H, Jiang Q, Wang Y, Zhang H, Wei Y, Xue W, Pu Z *et al*: **MicroRNA-497-5p Induces Cell Cycle Arrest Of Cervical Cancer Cells In S Phase By Targeting CBX4**. *Onco Targets Ther* 2019, **12**:10535-10545.
57. Mok MT, Zhou J, Tang W, Zeng X, Oliver AW, Ward SE, Cheng AS: **CCRK is a novel signalling hub exploitable in cancer immunotherapy**. *Pharmacol Ther* 2018, **186**:138-151.
58. Tadesse S, Caldon EC, Tilley W, Wang S: **Cyclin-Dependent Kinase 2 Inhibitors in Cancer Therapy: An Update**. *J Med Chem* 2019, **62**(9):4233-4251.
59. Zhang Q, Miao S, Han X, Li C, Zhang M, Cui K, Xiong T, Chen Z, Wang C, Xu H: **MicroRNA-3619-5p suppresses bladder carcinoma progression by directly targeting beta-catenin and CDK2 and activating p21**. *Cell Death Dis* 2018, **9**(10):960.
60. Xie B, Zhao Z, Liu Q, Wang X, Ma Z, Li H: **CircRNA has_circ_0078710 acts as the sponge of microRNA-31 involved in hepatocellular carcinoma progression**. *Gene* 2019, **683**:253-261.
61. Du WW, Yang W, Liu E, Yang Z, Dhaliwal P, Yang BB: **Foxo3 circular RNA retards cell cycle progression via forming ternary complexes with p21 and CDK2**. *Nucleic Acids Res* 2016, **44**(6):2846-2858.

Tables

Table 1 The clinical characteristics of patients with cervical cancer.

Characteristics	Case (30)
Age (years)	
≤ 55	13 43.3%)
> 55	17 (56.7%)
FIGO stage	
I-IIa	20 (66.6%)
IIb,III-IV	10 (33.3%)
Tumor size	
≤4 cm	18 (60.0%)
4 cm	12 (40.0%)
Lymph node	
Negative	18 (60%)
Positive	12 (40%)

FIGO, International Federation of Gynecology and Obstetrics.

Table 2. The primer sequences for RT-qPCR

Name	Primer sequences (5’-3’)
Circ_0084927	
Forward	CGAAGGAACGGAGAAGCTCT
Reverse	GTGCCCTGACTACGGTGTTA
Circ_0084912	
Forward	CTTGATGACCCCAGAAGGAG
Reverse	ATATTCCAGGCTTCCCAACC
Circ_0081723	
Forward	CCATCACCGACCTCATCAGT
Reverse	TGATGTTTCCCAGTGTGTGG
Circ_0106385	
Forward	GAGGAGGAGGAGAAGAATGC
Reverse	ACGTGGCACAGACCTCTCTC
Circ_0099591	
Forward	CCAACCAATGAGTCGAAGGT
Reverse	CTCGGAGTGTGAGGGATAGC
miR-1179	
Forward	GCGCGCAAGCATTCTTTCAT
Reverse	GTCGTATCCAGTGCAGGGTCCGAGGTATTCGCACTGGTACGAACCAACCA
U6	
Forward	CTCGCTTCGGCAGCACA
Reverse	AACGCTTCACGAATTTGCGT
CDK2	
Forward	CCAGGAGTTACTTCTATGCCTGA
Reverse	TTCATCCAGGGGAGGTACAAC
β-actin	
Forward	CATGTACGTTGCTATCCAGGC
Reverse	CTCCTTAATGTCACGCACGAT

Figures

A GSE102686

circBase	adj.P.Value	P. Value	logFC	Gene Symbol
has_circ_0106385	0.009578	1.07E-04	2.89	SPECC1
has_circ_0084927	0.024417	7.47E-04	2.46	ESRP1
has_circ_0099591	0.049748	2.89E-03	2.26	CDK17
has_circ_0081723	0.026032	9.17E-04	2.03	POLR2J2
has_circ_0084912	0.009578	1.50E-04	2.01	KIAA1429

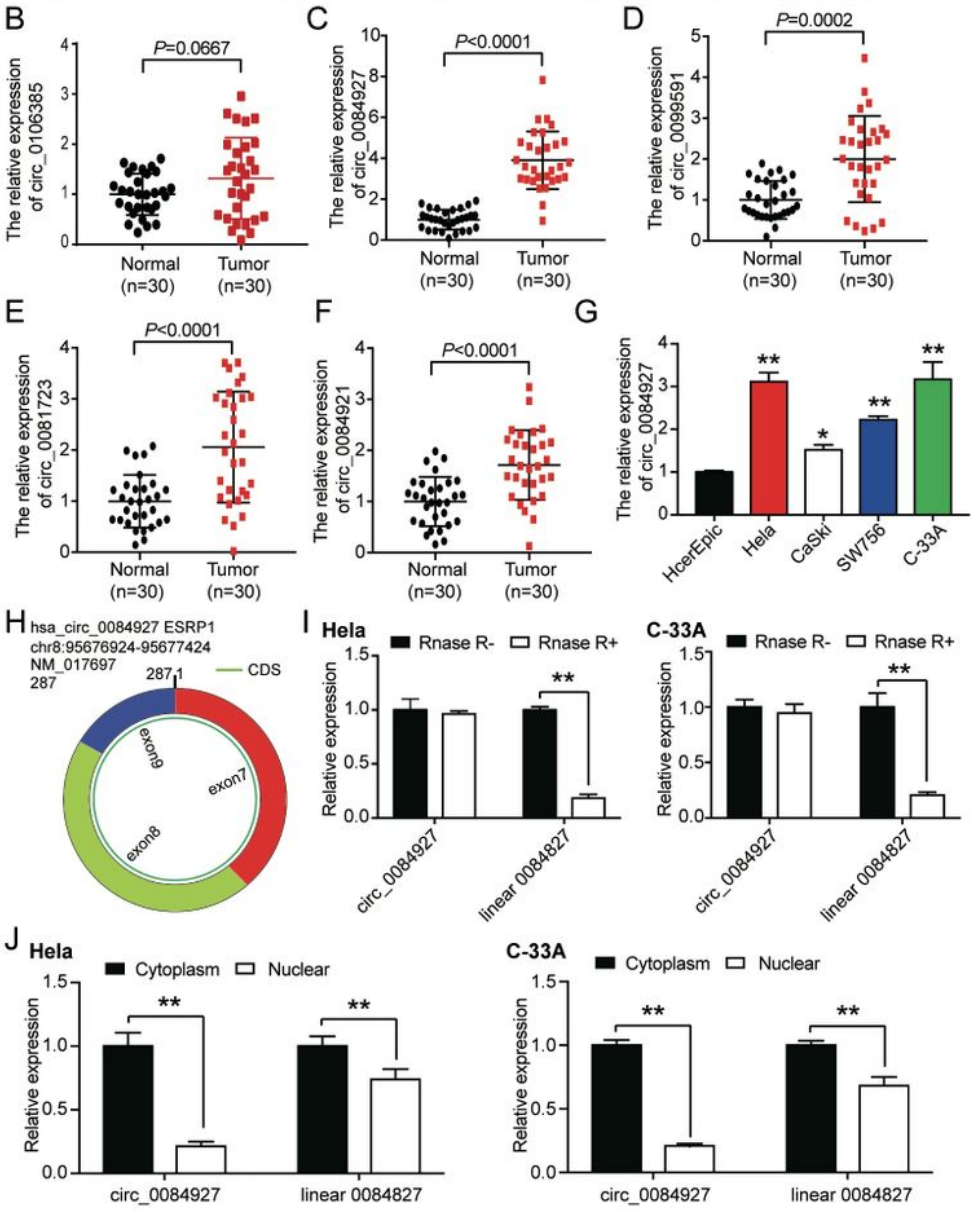

Figure 1

The identification of circRNA of interest and its characteristics. A. By analyzing GSE102686 data series, we identified 21 differentially expressed circRNAs in cervical cancer, and the top 5 most significantly overexpressed circRNAs were presented here. The criteria for differential expression was adj. P <0.05 and

log|FC|>=1.5. B-F. The qPCR results for the top 5 most significantly upregulated circRNAs in our collected tumorous cervical tissues and healthy adjacent tissues. N=30. G. qPCR results for the expression of circ_0084927 in selected cell lines. Except for HcerEpic cell line, the others are cervical cancer cell lines. *P<0.05, **P<0.01, compared with HcerEpic cell line. H. The structure of circ_0084927 was illustrated. It is formed with three exons 7-9 from ESRP1 host gene. I. The RNase R+ tolerance feature of circ_0084927 in Hela anc C-33A cell lines. **P<0.01, compared with the control group without Rnase R treatment. J. The localization of circ_0084927 in Hela and C-33A cell lines using a cell fractionation method. **P<0.01, compared with the level of circ_0084927 or linear ESRP1 mRNA in cytoplasm.

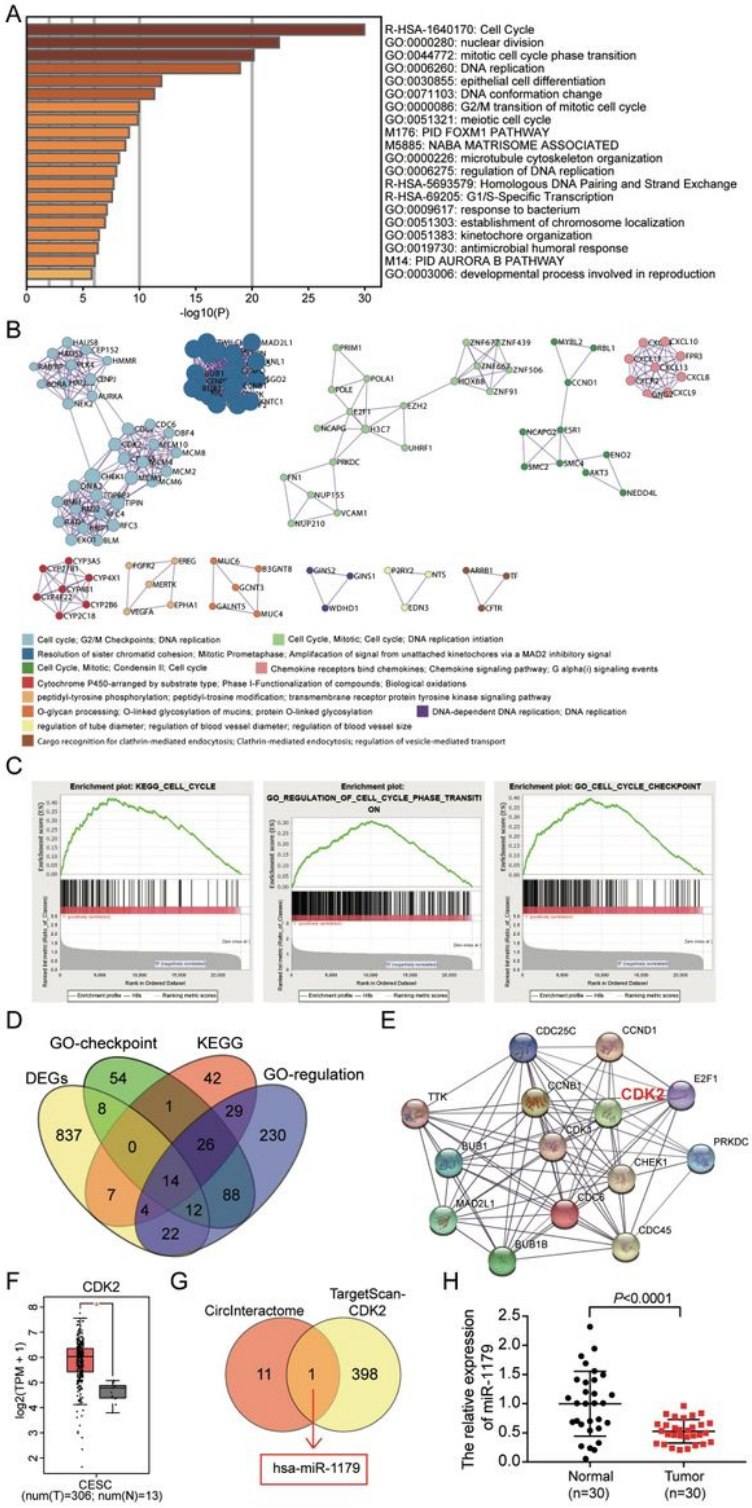

Figure 2

The identification of mRNA and miRNA of interest. A-B. The differentially expressed genes (DEGs) of GSE63514 data series went through the analysis of Metasacape.org. A is a bar graph showing the enriched terms across the 904 input DEGs list. The bar was colored by P values. B is the MCODE components identified in the input DEGs list. The criteria for DEGs were adj. P<0.01 and log|FC|>=2. C. GSEA analysis was done to DEGs of GSE63514 data series, and it was found that cell cycle-related terms

were significantly upregulated in cervical cancer. D. The DEGs that involved in the three GSEA datasets were screened out, and 14 of them went through STRING analysis (E). Among the genes in the STRING network, we noticed that CDK2 had been studied thoroughly in cervical cancer, however, its networking with circRNAs had been limitedly studied. Thus, CDK2 was chosen as our gene of interest in this study. F. GEPIA algorithm gave the relative expression of CDK2 in cervical squamous cancer (CESC). Num=number. T=tumor, N=healthy normal. G. The identification of miRNA that was sponged by circ_0084927 and targeted CDK2 mRNA. The downstream miRNAs of circ_0084927 was predicted by circular RNA interactome (https://circinteractome.nia.nih.gov/), and the upstream miRNAs of CDK2 mRNA were predicted by TargetScan Human 7.2. Finally, miR-1179 was identified. H. The relative expression of miR-1179 in our collected tissue samples.

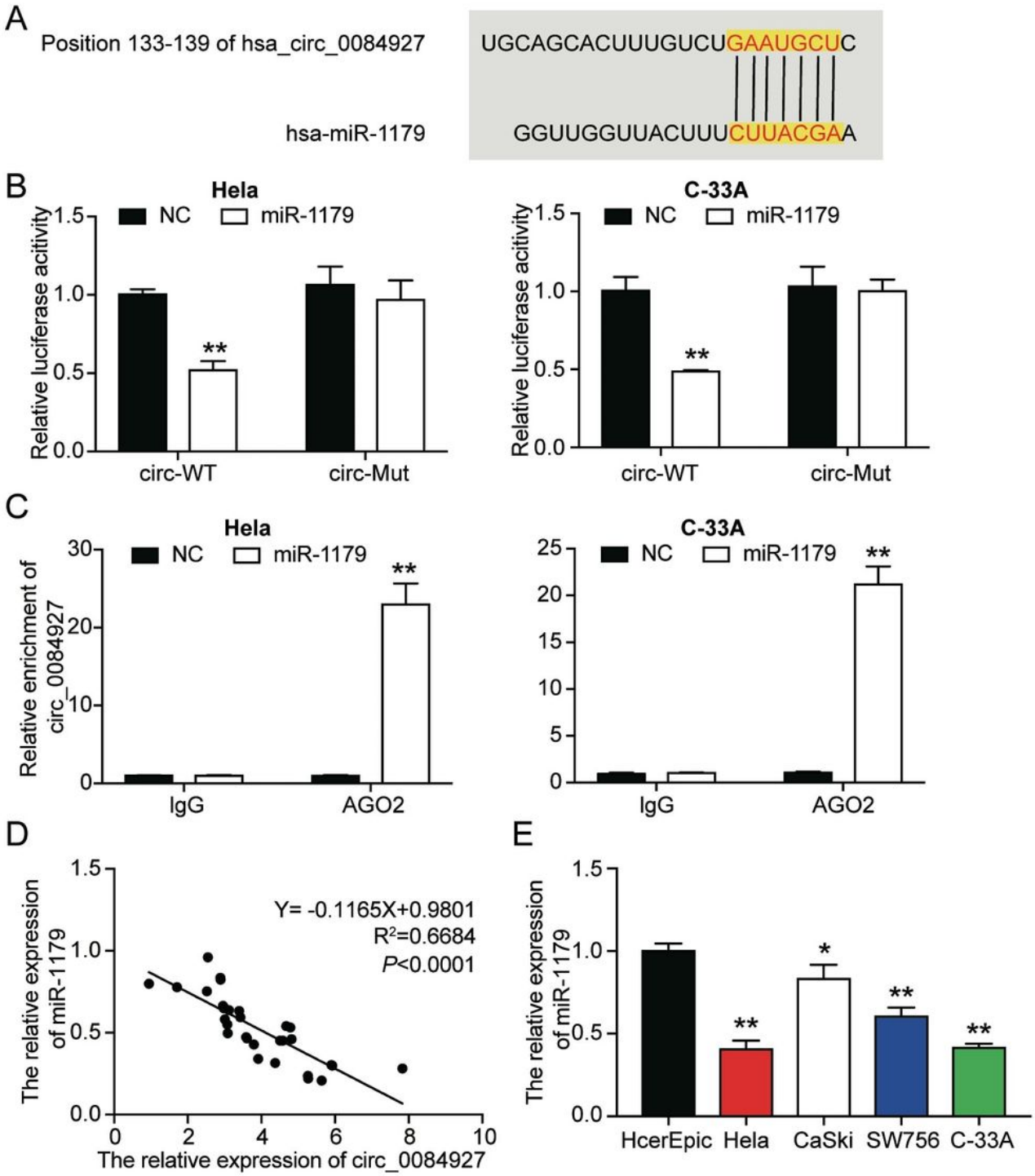

Figure 3

Circ_0084927 directly targeted miR-1179. (A) The scheme showed that circ_0084927 interacted with the 3'UTR oligonucleotide sequence of miR-1179. The binding relationship was predicted by circular RNA interactome. (B) Potential binding between circ_0084927 and miR-1179 was validated by dual-luciferase reporter assay. Circ_0084927 mutant or circ_0084927 wild-type plasmids containing fluorescein and miR-1179 mimic were co-transfected into HeLa cells and C-33A cells. **P< 0.01, compared with NC group. (C)

The interaction between circ_0084927 and miR-1179 was measured by RIP analysis. IgG was the negative control for AGO2. NC was the negative control for miR-1179 mimic. **P< 0.01, compared with NC group. (D) The expression of miR-1179 in cervical cancer tissues was tested by qRT-PCR, with U6 as an internal control. A negative correlation relationship between circ_0084927 and miR-1179 expression was identified by spearman correlation analysis. (E) The expression of miR-1179 in cell lines. *P< 0.05, **P< 0.01, compared with HcerEpic cell line, which is a control cell line. (B-E) The data were in the form of mean ±SD of three experiments.

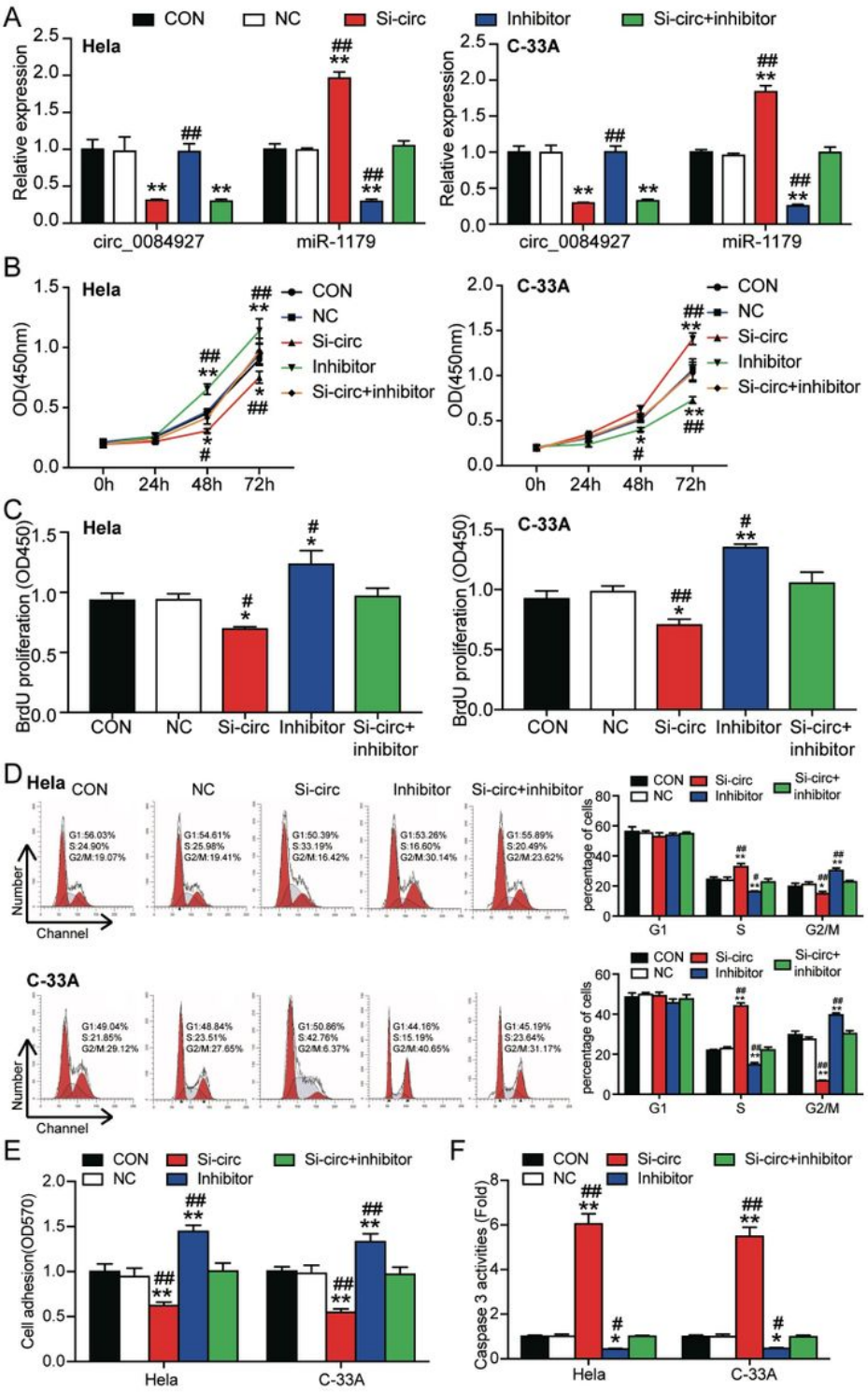

Figure 4

Circ_0084927 enhanced cervical carcinogenesis by inhibiting miR-1179. (A) Transfection efficiency of si-circ_0084927 and miR-1179 inhibitor in transfected cells was detected by qRT-PCR. (B) The proliferation of HeLa and C-33A cells transfected with si-NC, si-circ_0084927, miR-1179 inhibitor or si-circ_0084927 plus miR-1179 inhibitor was determined by CCK-8 assay. (C) BrdU incorporation assay was used to analyze the proliferation of HeLa and C-33A cells transfected with si-NC, si-circ_0084927, miR-1179 inhibitor or si-circ_0084927 plus miR-1179 inhibitor. (D) Cell cycle progression of HeLa and C-33A cells transfected with si-NC, si-circ_0084927, miR-1179 inhibitor or si-circ_0084927 plus miR-1179 inhibitor was identified by flow cytometry assay. (E) Cell-matrix adhesion assay was used to determine the adhesion ability of HeLa and C-33A cells transfected with si-NC, si-circ_0084927, miR-1179 inhibitor or si-circ_0084927 plus miR-1179 inhibitor. (F) The apoptosis of HeLa and C-33A cells transfected with si-NC, si-circ_0084927, miR-1179 inhibitor or si-circ_0084927 plus miR-1179 inhibitor was determined by caspase 3 activation experiment. (A-F) The data were in the form of mean ±SD of three experiments. *P< 0.05, **P< 0.01, compared with CON (blank control) group; #P< 0.05, ##P< 0.01, compared with si-circ (circ_0084927 siRNA) group.

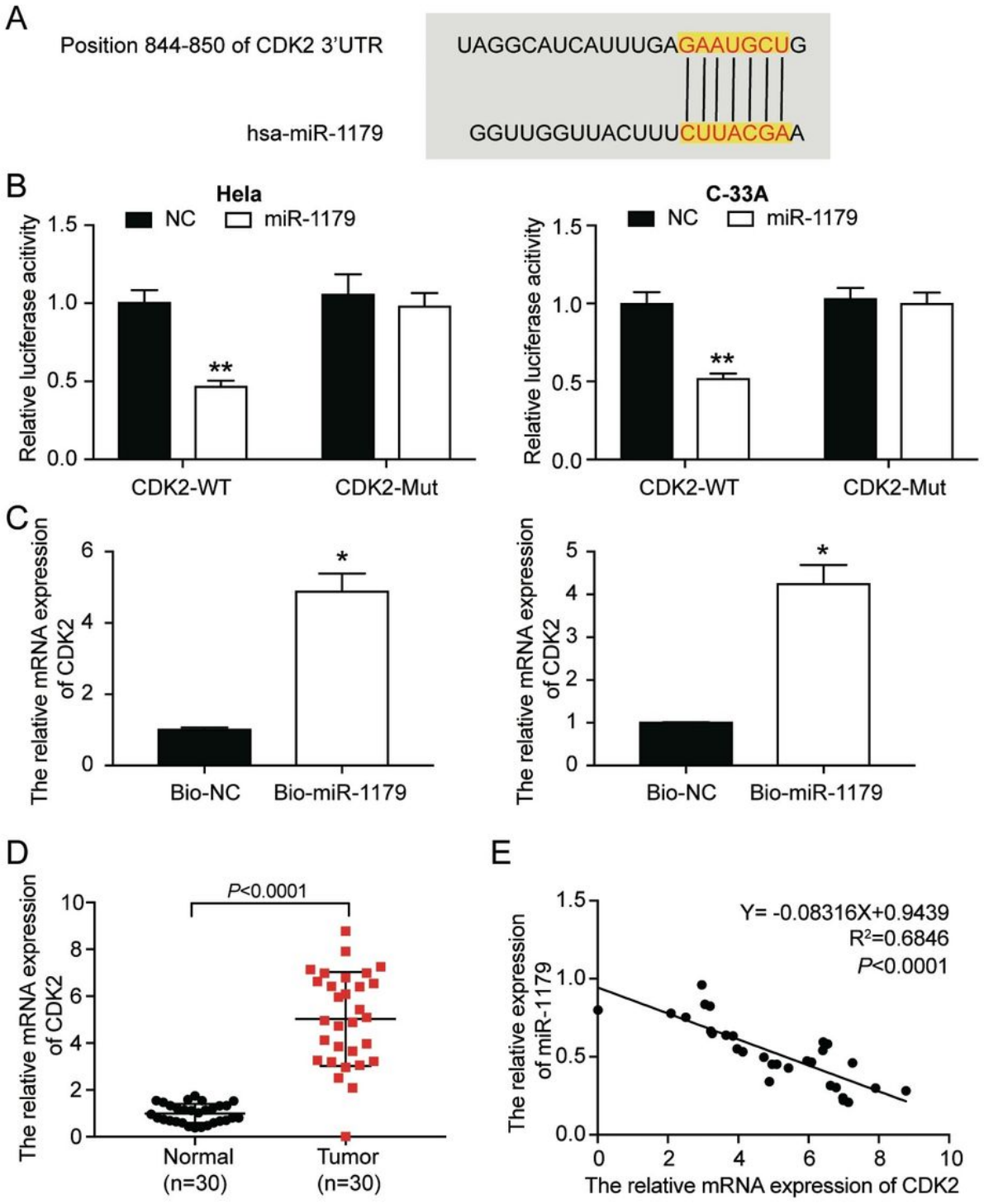

Figure 5

MiR-1179 directly inhibited CDK2 mRNA expression by binding to its 3'UTR. (A) Potential binding site between miR-1179 and CDK2 was predicted by TargetScan Human 7.2. (B) Potential binding between miR-1179 and the 3'UTR of CDK2 gene was validated by the luciferase reporter gene assay. CDK2 mutant or CDK2 wild-type plasmids containing fluorescence group and miR-1179 were co-transfected into HeLa and C-33A cells. **P< 0.01, compared with NC group. NC=negative control. (C) RNA pull-down assay was

used to validate the interaction between CDK2 mRNA and miR-1179. Bio=biotin-labelled. *P< 0.05, compared with bio-NC group. (D) CDK2 expression in CC tissues and normal tissues was detected by qRT-PCR. (E) The correlation between miR-1179 and CDK2 expression was identified by spearman correlation analysis. (B-E) The data were in the form of mean ±SD of three experiments.

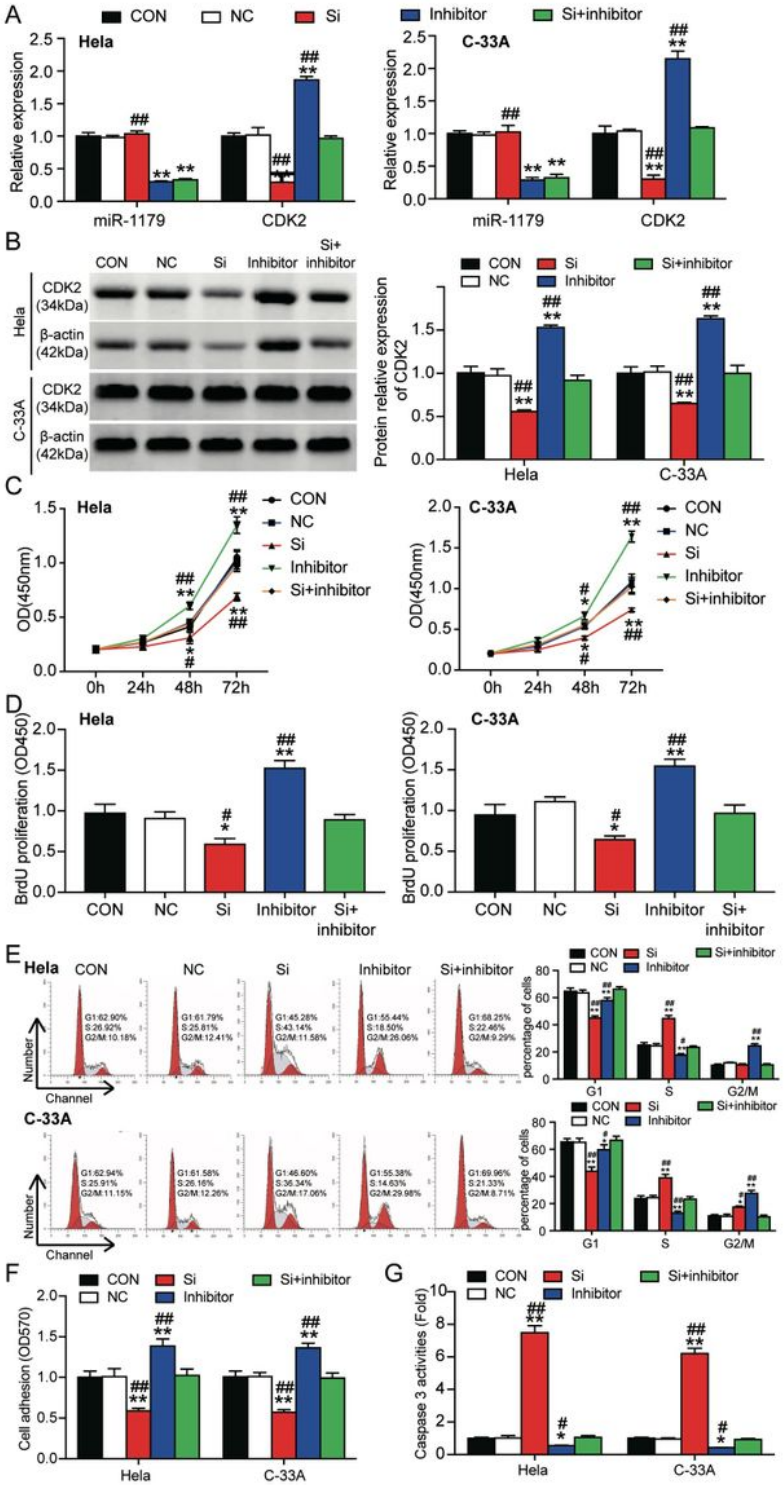

Figure 6

Circ_0084927 promoted cervical carcinogenesis by sponging miR-1179 that suppressed CDK2. (A) The transfection efficiency of HeLa and C-33A cells was measured by qRT-PCR. CON: blank control; NC: negative control; Si: CDK2 siRNA; inhibitor: miR-1179 inhibitor. (B) Western blotting of CDK2 in transfected HeLa and C-33A cells was used to reflect transfection efficiency at protein level. (C) CCK-8 assay was used to determine the proliferation of transfected HeLa and C-33A cells. (D) The proliferation of transfected HeLa and C-33A cells was determined by BrdU assay. (E) Cell cycle progression of transfected HeLa and C-33A cells was identified by flow cytometry assay. (F) Cell-matrix adhesion assay was used to determine the adhesion ability of transfected HeLa and C-33A cells. (G) The apoptosis of the transfected HeLa and C-33A cells was determined by Caspase 3 activation experiment. (A-G) NC, CDK2 siRNA, miR-1179 inhibitor or CDK2 siRNA plus miR-1179 inhibitor were transfected into HeLa and C-33A cells. The data were in the form of mean ±SD of three experiments. *P< 0.05, **P< 0.01, compared with CON group, and #P< 0.05, ##P< 0.01, compared with Si group.